Waste Management 114 (2020) 341–350

Contents lists available at ScienceDirect

Waste Management

journal homepage: www.elsevier.com/locate/wasman

Steam gasification of lignite and solid recovered fuel (SRF) in a bench scale fluidized bed gasifier

Elisa Savuto [a,*], Andrea Di Carlo [b], Katia Gallucci [b], Andrea Di Giuliano [b], Sergio Rapagnà [a]

[a] University of Teramo, Via R. Balzarini 1, 64100 Teramo, Italy
[b] University of L'Aquila, Via Campo di Pile, L'Aquila, Italy

ARTICLE INFO

Article history:
Received 24 February 2020
Revised 6 July 2020
Accepted 8 July 2020
Available online 18 July 2020

Keywords:
Lignite gasification
Waste gasification
Solid Recovered Fuel
Fluidized bed gasifier

ABSTRACT

The reduction of CO_2 emissions and solid waste disposal are critical issues with high importance for the environmental protection. Gasification is a promising process for sustainable energy production, because it can produce a versatile gaseous fuel starting from a wide range of organic feedstocks, and with reduced greenhouse gas emissions compared to combustion. Lignite is an abundant carbonaceous resource in Europe and in this work, gasification tests were carried out with lignite and a lignite and Solid Recovered Fuel (SRF) mixture, to evaluate the quality of gas produced from co-gasification of waste materials, in view of the final uses of the gas. Experimental gasification tests were carried out in a bench scale fluidized bed gasifier at different operating temperatures; the results were evaluated in terms of gas composition, tar content and conversion rates. In addition, characterization analyses were carried out on materials before and after the tests, and pressure fluctuation signals were analysed in order to evaluate the fluidization quality of the bed inventory.

1. Introduction

The reduction of fossil CO_2 emissions and the valorisation of waste materials are crucial goals to reduce the effects of climate change (Meylan et al., 2015; Singhabhandhu and Tezuka, 2010). Attention is thus being focused on sustainable routes for energy production such as gasification, a very promising process that can be used instead of combustion for the production of energy from carbon-based materials, such as lignite, which is a very abundant resource in Europe (European Association for Coal and Lignite, n.d.). Gasification is a process able to convert solid organic materials to produce an H_2-rich gaseous fuel. The product gas generated from gasification is a versatile fuel that can be exploited for a wide range of final uses, such as the production of electricity in integrated gasification combined cycle systems (IGCC) or in fuel cells, or for the synthesis of liquid fuels, i.e. Fischer-Tropsch or methanol synthesis (Venvik and Yang, 2017; Wang et al., 2017).

In 2016, 2.01 billion tonnes of solid waste were generated worldwide, and the annual waste production is expected to increase up to 3.40 billion tonnes by 2050 (The World Bank, 2019). Moreover, around 45.7% of the wastes generated in EU in 2016 were disposed of in landfills (Eurostat, 2019); it is thus evident that the issues of management, recycling and valorisation of waste have to be tackled (Bosmans et al., 2013; Hervy et al., 2019).

An interesting option of feedstock for the gasification process could be to combine lignite (with its advantageous features of high heating value and low volatiles content) with solid waste (Pinto et al., 2003), in order to integrate waste disposal and valorisation into energy production technologies. Municipal Solid Waste (MSW), which is in fact a resource exploitable for energy production (Arena, 2012; Belgiorno et al., 2003; Lombardi et al., 2015), can be processed into Solid Recovered Fuel (SRF), a fuel with a fairly homogeneous composition intended for use in energy recovery facilities (Patel et al., 2012).

For blended feedstocks with generally high ash content, as in the case of lignite and SRF, an appropriate gasification technology must be chosen, to avoid technical issues. For this process, the fluidized bed technology can be a suitable solution (Arena et al., 2015), because it provides high conversion rates, high fuel flexibility, and operating temperatures that are generally below the ash melting point.

Abbreviations: Avg, Average; b.p., bottom product; EDS, Electron Dispersive X-ray Spectrometry; GC-MS, Gas Chromatograph with Mass Spectrometer; HPLC, High Performance Liquid Chromatography; HTW, High Temperature Winkler; IGCC, Integrated gasification combined cycle; MSW, Municipal Solid Waste; PSDF, Power Spectral Density Function; S/F, Steam to Fuel; SEM, Scanning Electron Microscope; SRF, Solid Recovered Fuel; XRF, X-ray Fluorescence.

* Corresponding author.
E-mail address: esavuto@unite.it (E. Savuto).

https://doi.org/10.1016/j.wasman.2020.07.016
0956-053X/

Nomenclature

Symbols

$d_{3,2}$	Average particle diameter from particle size distributions
$F_{gas,out}$	Total dry N_2-free volume gas flow rate produced
$F_{fuel,in}$	Mass flow rate of the input fuel in the gasifier
$\dot{m}_{water,in}$	Mass flow rate of water input
$\dot{m}_{water,out}$	Mass flow rate of water output
n_i	Moles of the i carbonaceous species in the product gas (CO, CO_2, CH_4),
$n_{C_{in}}$	Total moles of C in the feedstock input
Y_{gas}	Gas yield
Xc	Carbon conversion
η_{wc}	Water conversion

Other works have reported experimental results of gasification tests of SRF in fluidized bed reactors at different operating conditions: at laboratory scale (Recari et al., 2016), in a pilot scale reactor (Arena and Di Gregorio, 2014), evaluating waste materials with different compositions (Arena et al., 2010; Arena and Di Gregorio, 2016), and also blending SRF with biomass wastes (Pinto et al., 2014). However, few studies have been focused on steam gasification of SRF (pure or in blends) in fluidized bed reactors, in which the process could benefit from the advantages of the operating conditions: the high flexibility of fluidized bed technology and the high conversion rates obtained with steam gasification. The aim of the present work is to carry out steam gasification tests of both lignite and a blend of lignite and SRF (80 wt%-20 wt% respectively) in a bench scale fluidized bed reactor, using lignite ash as bed material. The mixing of waste with lignite is intended to exploit its above mentioned features in order to obtain a high quality syngas, although starting from a blend with a low quality fuel. The bed material used is the bottom product of the High Temperature Winkler (HTW) gasifier (Krause et al., 2019), residual product of lignite gasification thus with a high content of ash, which can have a beneficial effect on the gasification process (Yip et al., 2010).

The present work was carried out within the European project LIG2LIQ (G.A. n°796585, 2018), in which the objective is to develop of an economically efficient process for the production of liquid fuels (Fischer-Tropsch fuels or methanol) from lignite and SRF, by means of the HTW gasification technology. Initially, the process of simple lignite HTW gasification was optimized in the same laboratory scale fluidized bed reactor (Savuto et al., 2020); in this phase steam gasification experiments were carried out with the mixture of lignite and SRF, using the lignite residual bottom product as bed material in order to reproduce the HTW process at a laboratory scale.

Different operating temperatures (750, 800, 850 °C) were adopted in the experimental tests, in order to study the best conditions to produce a high-quality syngas; the results were evaluated in terms of syngas composition, tar content, gas yield and conversion rates. The results obtained were analysed to deduce the best operating conditions to obtain a product gas with low tar content and high H_2 and CO fractions, suitable for the downstream processes of Fischer-Tropsch or methanol synthesis.

2. Materials and methods

2.1. Experimental test rig

The experimental apparatus is composed of a stainless steel cylindrical bubbling fluidized bed gasifier (internal diameter 100 mm and height 850 mm) externally heated by means of a 6 kW electric furnace. Steam was used as gasification agent and a flow of N_2 was added in order to fluidize the bed; they were fed from the bottom of the gasifier by percolation through a porous ceramic plate. The gas residence time, estimated from the input flows and the volatile fraction of the feedstock, is approximately 0.95 s in the bed and 3.10 s in the freeboard. In previous work carried out with the same experimental set-up and similar operating conditions (Savuto et al., 2019) the gas compositions obtained were close to the thermodynamic equilibrium compositions, proof that the residence times are appropriate to guarantee the gasification of the solid feedstock in the bed, and the reforming reactions in gas phase in the freeboard (Basu, 2006).

The bed material used was HTW (High Temperature Winkler) bottom product, a solid residue composed by char and ash produced from the gasification of lignite in the HTW reactor (Herdel et al., 2017). The height of the bed in the reactor was approximately 200 mm. The feedstock, consisting of pre-dried Rhenish lignite supplied by RWE AG, simple or mixed with Subcoal® (SRF supplied by N + P (N+P Subcoal®)), was fed continuously into the reactor bed by means of a screw feeder and a feeding probe. The feeding probe was purged with a small N_2 flow of 2 Nl/min, in order to help the fall of the feedstock and to avoid the material from clogging the tube. A porous ceramic candle was installed in the upper part of the freeboard inside the reactor; the aim of the candle is to filter the solid particulate from the product gas, that is forced to pass through the filter in order to exit the gasifier.

Downstream from the gasification reactor, the product gas flows through a series of heat exchangers in order to condense and separate the unreacted water; the flow rate and composition of the dry product gas stream were measured by means of mass flow meters and gas analysers. A slipstream of the product gas was used for tar sampling according to the technical specification CEN/TS 15439.

Temperatures were measured by three K-type thermocouples, one in the reactor bed (T1), one in the freeboard (T2) and another at the head of the candle, just at the outlet of the filter cavity (T3). The operating temperature was assumed as the average value of the temperatures measured in T1, T2 and T3. Pressure drops through the candle (ΔP1) and through the reactor (ΔP2) were measured by pressure probes located at different points in the reactor.

Pressure fluctuation signals inside the gasifier were also acquired, with a vertical probe in the freeboard, connected to a pressure transducer (P/E); each signal was then amplified, digitally converted and stored in a PC. The frequency of data acquisition was 100 Hz, much higher than those typically observed in the gas-fluidised bed under study (less than 10 Hz); the duration of each acquisition was of 2–3 min, to ensure their repeatability and significance (Gallucci et al., 2002). Signals were processed and analysed to obtain their power spectral density functions (PSDF) by fast Fourier transform (Gallucci and Gibilaro, 2005); in this way the frequency of the erupting bubbles can be estimated and the fluidization quality of the bed can be evaluated. A scheme of the experimental set-up can be found in Fig. 1.

The test campaign was carried out using HTW bottom product as bed material, with fixed values of feedstock and steam feeding rates, in order to have a Steam/Fuel ratio always equal to 0.5 (g/g). The value of steam/fuel was chosen in compliance with the typical values used for steam gasification reactions, usually chosen between 0 and 1, as reported in literature (Karimipour

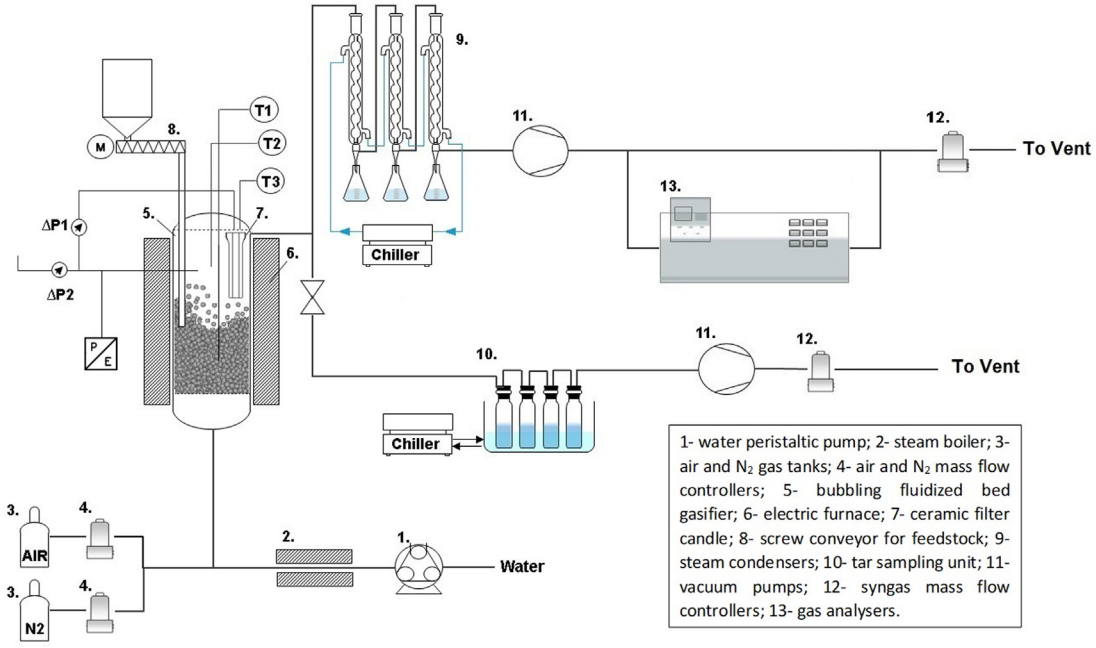

Fig. 1. Scheme of the experimental gasification test rig.

et al., 2013; Pinto et al., 2003; Tursun et al., 2013); moreover, higher steam/fuel ratios could enhance conversion rates but will cause a decrease in the gasifier efficiency. Some operating parameters were changed in the experimental tests: the temperature ranged between 750 and 850 °C, while the feedstock was simple lignite or a mixture of lignite (80 wt%) and SRF (20 wt%). The proportion 80%-20% was chosen for the first waste co-gasification test campaign in our bench scale experimental set-up; the moderate percentage of waste in the feedstock was chosen to avoid possible issues related to SRF and its heterogeneous composition (for example clogging of the feeding probe, ash melting in the bed etc.). Operating temperatures of tests #1, #2 and #3 were 750, 800 and 850 °C respectively, with lignite as solid feedstock; tests #4, #5 and #6 were carried out at the same conditions adopted in those first 3 tests, but using the mixture of 80 wt% lignite and 20 wt% SRF as feedstock.

2.2. Analysis of products

A slipstream of approximately 1 Nl/min of the dry, cooled product gas was sent to online analysers for the evaluation of the gas composition. Online analysers allow detecting H_2, CO, CO_2, CH_4, H_2S and NH_3 (ABB URAS, LIMAS, CALDOS and ULTRAMAT 6 Siemens).

The water content in the product gas was calculated from the quantity of water collected in the flasks connected to the steam condensers. The water conversion $\eta_{wc}(\%)$ was thus calculated as:

$$\eta_{wc} = \frac{\dot{m}_{water,in} - \dot{m}_{water,out}}{\dot{m}_{water,in}} \text{x}100 \quad (1)$$

where $\dot{m}_{water,in}$ and $\dot{m}_{water,out}$ are the mass flow rates of water input and output, respectively.

The dry product gas flow rate, measured by means of a mass flow rate controller, allowed calculating the gas yield $Y_{gas}(Nm^3/kg_{feedstock})$:

$$Y_{gas} = \frac{F_{gas,out}}{F_{feedstock,in}} \quad (2)$$

where $F_{gas,out}$ is the total dry N_2-free volume gas flow rate produced, and $F_{feedstock,in}$ is the mass flow rate of the input feedstock.

By measuring of the product gas composition and the carbon content in the feedstock, together with their flow rates, it was possible to calculate the carbon conversion $Xc(\%)$:

$$Xc = \frac{n_{CO} + n_{CO_2} + n_{CH_4}}{n_{C_{in}}} \text{x}100 \quad (3)$$

where n_i are the moles of the i carbonaceous species in the product gas (CO, CO_2, CH_4), and $n_{C_{in}}$ are the total moles of C in the feedstock input.

The tar samples, collected by impinger bottles in the tar sampling unit, were analysed offline in a GC-MS (GC7890A Agilent with a MSD-Triple Axis Detector 5975C) and in a HPLC (Hitachi "Elite LaChrom" L-2130) for the identification and quantification of the tar compounds in the product gas.

3. Results and discussion

3.1. Analysis of materials

The main materials used in the experimental tests are lignite, HTW bottom product and SRF. The particle size distribution of lignite and HTW bottom product before use are reported in Fig. 1**S**. The average $d_{3,2}$ diameters of lignite and HTW bottom product before use given by the particle size analysis are 20.66 and 441.93 μm, respectively.

The particle size distribution of SRF, carried out with sieves, is reported in Table 1**S**. The average $d_{3,2}$ diameter of SRF resulting from the particle size analysis is 1836 μm.

The characterization analyses of lignite and SRF, supplied by ICHPW, and of the HTW bottom product before use are reported in Table 1.

The CHNS analysis of HTW bottom product before use, which is the solid residue produced in the Winkler gasifier, shows that it has still a very high carbon content, despite the high C conversion rate. The inorganic ash content, equal to 9.48 wt%, was measured according to the standard ISO 1171:2010 (ISO, 2010).

Table 1
Characterization analyses of lignite, SRF and HTW bottom product.

	Lignite	SRF	HTW b. p. before use	HTW b. p. after use
Total Moisture content (wt %)	10.60	3.30	–	–
Ash content (dry basis) (wt %)	3.80	14.40	9.48	34.32
Volatile matter (dry basis) (wt %)	50.31	76.30	–	–
C (dry basis) (wt %)	67.30	53.70	74.35	71.66
H (dry basis) (wt %)	4.79	7.56	1.32	0.22
N (dry basis) (wt %)	0.84	0.59	0.09	0.02
S (dry basis) (wt %)	0.35	0.21	0.52	0.65
Cl (dry basis) (wt %)	0.022	1.93	–	–
O* (dry basis) (wt %)	26.70	36.01	23.72	27.45

*Oxygen content is calculated by difference

The HTW bottom product was analysed with SEM/EDS before being used as bed material in the gasification reactor (Fig. 2): a shell-type structure with several holes appeared; the micro-analysis highlights the presence of C in the structure, and Mg and Ca as typical elements contained in the ashes. The morphology observed by SEM could be related to the process of formation of the ash in the HTW gasifier, in which O_2 is used (together with steam) (Herdel et al., 2017; Krause et al., 2019), that could have caused a fast release of the gases from the material, thus creating the shell-shape structure.

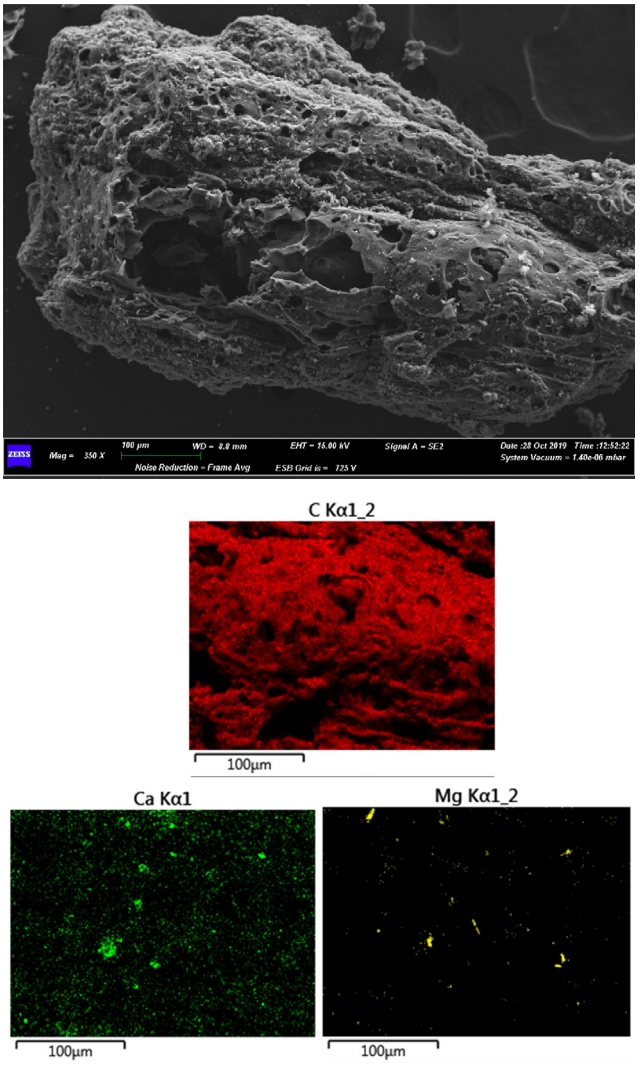

Fig. 2. SED/EDS of HTW bottom product before use (350x).

Samples of lignite ash and SRF ash were analysed by ICP-OES, in order to identify the inorganic compounds present in the feedstocks and in the HTW bottom product used as bed material; the results are shown in Table 2**S**.

3.2. Gasification results

Each of the gasification tests was carried out continuously, without interruptions or changes in the configuration. The steady-state was reached after some minutes, as proofed by the gas compositions and flow rates acquired online, which showed constant values during the tests. Even though the bed material has a high content of carbon, the results show that smooth gasification of the continuously fed material took place, therefore allowing to obtain a steady-state gasification process. Moreover, the weight of the bed material extracted from the reactor after each test was approximately the same of the quantity inserted before the test, further proof that the steady-state was reached in the experimental runs.

Fig. 2**S** shows the time resolved gas species and gas flow rates, analysed online during test #2 and test #5, as representative cases; for the other tests the trend during the time was similar, showing no relevant variations in the results analysed online.

The results obtained from the gasification tests are shown in Table 2.

The values chosen as operating temperatures were 750, 800 and 850 °C; in Table 2 the measured values of temperatures during each test are shown, just a few degrees (°C) different from the set points chosen.

The results displayed in Table 2 show that for higher temperatures, the gas yield and the in H_2O and C conversions are increased, while CH_4 and tar content is decreased. The H_2 vol% in the dry N_2 free gas is decreased for tests at higher temperature, however the H_2 production in terms of Nl/min is increased. This is due to increased gas yield at higher temperatures, so in the higher volume of total gas produced, despite the slightly lower percentage of H_2, the total Nl of H_2 produced in relation to the unit mass of feedstock, or time, is actually increased.

Anincrease of CO and decrease of CO_2 is also observed at higher temperatures probably caused by a combination of a reduced extent of the WGS reaction, and the Boudouard reaction (CO_2 + C → 2CO) that would combine the CO_2 in the gas with the C in the bed material, to produce CO (Lahijani et al., 2015). Furthermore, the higher contents of CO and H_2 could also be caused by the gasification of some of the C contained in the bed material. Both the reactions described are indeed favoured with the increase of temperature, which is consistent with the different gas compositions observed at 750, 800 and 850 °C (Table 2).

Tests carried out withthe blend of lignite and SRF (#4, #5, #6 in Table 2) gave in general similar results to the corresponding test with only lignite (#1, #2, #3 in Table 2). Only slight differences appeared in the presence of SRF: the gas composition showed

Table 2
Results of gasification tests.

Test	#1	#2	#3	#4	#5	#6
Feedstock		Lignite			Lignite + SRF	
Feeding rate (g/min)		12.9			10.4	
Bed Temperature (°C)	745 ± 1.3	802 ± 2.0	841 ± 6.8	759 ± 2.3	802 ± 3.3	843 ± 1.3
Avg Temperature (°C)	757 ± 1.6	806 ± 1.5	843 ± 5.0	751 ± 2.2	797 ± 3.6	844 ± 1.4
Steam/Fuel (g/g)	0.52	0.51	0.50	0.58	0.58	0.57
Test duration (min)	58	51	47	59	60	58
H_2O conversion (%)	71.03	84.13	94.62	69.83	85.32	85.51
C conversion (%)	48.31	64.17	68.71	55.59	65.73	74.73
Gas yield (Nm^3/kg_{daf})	1.42 ± 0.13	1.73 ± 0.15	1.79 ± 0.19	1.50 ± 0.09	1.69 ± 0.16	1.94 ± 0.12
H_2 (vol%) dryN_2free	56.34 ± 0.75	54.61 ± 0.74	53.61 ± 1.06	56.35 ± 1.78	54.74 ± 2.07	54.76 ± 1.87
CO (vol%) dryN_2free	27.32 ± 1.51	35.64 ± 0.84	40.33 ± 0.84	25.12 ± 0.74	33.57 ± 0.95	35.40 ± 1.14
CO_2 (vol%) dryN_2free	14.04 ± 0.61	7.66 ± 0.39	4.18 ± 0.42	14.21 ± 0.49	8.48 ± 0.49	6.53 ± 0.63
CH_4 (vol%) dryN_2free	2.29 ± 0.22	2.09 ± 0.23	1.88 ± 0.19	4.32 ± 0.44	3.21 ± 0.38	3.31 ± 0.31
H_2S (ppm) dryN_2free	636 ± 37	143 ± 15	114 ± 10	1663 ± 135	502 ± 54	555 ± 45
NH_3 (ppm) dryN_2free	1792 ± 71	1620 ± 86	756 ± 49	1360 ± 100	1696 ± 126	1232 ± 94
H_2 (Nl/min)	9.11	11.24	11.53	8.25	9.10	10.32
H_2 ($Nl/g_{feed\ daf}$)	0.82	1.01	1.03	0.74	0.82	1.16
Tar content HPLC (mg/Nm^3)	2140	1176	815	2831	940	1751
Tar content GC-MS (mg/Nm^3)	2144	433	220	2509	638	809
Mass balance (err %)	19.06	15.94	18.36	14.62	18.35	11.75

lower CO content and higher CH_4 and CO_2 contents, probably related to the plastic fraction of the SRF (Arena et al., 2015; Hervy et al., 2019). In particular, the higher production of light hydrocarbons, such as CH_4 in tests #4 to #6, could be related to the decomposition of more complex hydrocarbons present in the plastic materials contained in the SRF, as confirmed by (Pinto et al., 2007). Moreover, the composition of SRF that has a higher content of elemental oxygen compared to lignite (see Table 1) is likely the cause of the higher production of oxidized compounds in the syngas, such as CO_2, whose production is 1.19 Nl/min in test #6 and 0.85 Nl/min in test #3.

Comparing tests #3 and #6, the production of H_2 seems to be lower in test #6 however, considering the lower feed rate and the higher ash content of SRF, the comparison of H_2 production should be more correctly evaluated in terms of Nl per unit mass of feedstock dry and ash free (daf); in this way it is possible to observe that the H_2 production is slightly higher in test #6.

H_2O conversion is lower in test #6 compared to test #3, probably because of the difference in feed rates that causes a slightly higher S/F ratio for test #6, maybe resulting in excessive steam for the relative feedstock. Despite the lower H_2O conversion, the higher H_2 content observed in test #6 could be the proof of the release of H_2 from SRF, that in fact has a higher hydrogen content compared to lignite (see Table 1), and a higher reactivity, as shown by the higher gas yield. Moreover, the higher H_2 production could be related to dehydrogenation and cracking reactions of the SRF matrix (Chen and Yan, 1986; Qin et al., 2015).

The observations made regarding the influence of temperature on the gas quality can also be applied to the tests with lignite and SRF.

The best results for gasification of lignite were obtained at 850 °C (test #3 in Table 2), with 54 vol% of H_2 and 40 vol% of CO on a dry N_2 free basis, and a gas yield of 1.79 Nm^3/kg_{daf}. Similarly, for gasification of lignite and SRF, the test carried out at 850 °C (test #6 in Table 2) gave H_2 55 vol% and CO 35 vol% on a dry N_2 free basis, and a gas yield of 1.94 Nm^3/kg_{daf}.

The NH_3 content in tests with only lignite (#1, #2, #3 in Table 2) at 750 °C and 800 °C has values around 1800 ppm and 1600 ppm on dry N_2-free gas, respectively. At 850 °C, the content of NH_3 is much lower than the previous values, around 750 ppm. However, the total amounts of NH_3 produced per mass unit of feedstock are 1.75E-3, 2.16E-3 and 1.14E-3 $Nl_{NH3}/g_{feedstock}$ for tests at 750, 800 and 850 °C, respectively.

NH_3 in the tests with SRF and lignite (#4, #5, #6 in Table 2) showed values in the same order of magnitude of those obtained in the tests without SRF, around 1000–2000 ppm. It is observed that, similarly to the previous tests, NH_3 content is the highest at 800 °C, equal to 1696 ppm. The amounts of NH_3 per mass unit of feedstock are 1.73E-3, 1.89E-3 and 1.43E-3 $Nl_{NH3}/g_{feedstock}$ obtained at 750, 800 and 850 °C, respectively.

It is thus observed that the NH_3 content has its highest value at 800 °C, and then decreases for higher temperature, as also observed by Xie at al. in gasification experiments on coal macerals (Xie et al., 2005). It is possible that the trend noticed results from the combination of two effects related with increasing temperature: the higher production of NH_3 from the N-containing structures in coal enhanced in steam gasification (Chang et al., 2006; Li and Tan, 2000; Tian et al., 2007) and the thermal decomposition of NH_3, as found in literature (Zhou et al., 2000).

The H_2S content measured in the test carried out at 750 °C with simple lignite has an average value of 630 ppm, on dry N_2-free gas; in the tests with simple lignite at higher temperatures, the H_2S content is much lower, 143 ppm at 800 °C and 114 ppm at 850 °C. It seems that, for temperatures higher than 800 °C, the H_2S concentration in the gas is greatly decreased. The H_2S content in the tests with SRF has a very similar trend to that observed for the tests with simple lignite, with generally higher values; the content is the highest at 750 °C, around 1660 ppm, and it greatly decreases for higher temperatures, down to values of approximately 500 ppm, as also found in literature (Borgwardt, 1984),. In the literature (Galloway et al., 2015; Hu et al., 2006), CaO contained in the ash of the bed material has a good affinity with H_2S, that probably causes the reaction $CaO + H_2S \rightarrow CaS + H_2O$, which would allow the retention of S in the ashes and the decrease of H_2S in the syngas. The presence of CaO in the bed material is witnessed by the ICP-OES analyses of lignite ash and SRF ash (Table 2**S**), both showing an evident concentration of Ca; these results support therefore the hypothesis of the S retention in the ashes by means of the Ca compounds. The above mentioned reaction is inhibited by the presence of H_2O; in the tests at higher temperatures, the H_2O conversion is much higher and the residual steam in the syngas is lower; this could cause a higher extent of the reaction between CaO and H_2S thus explaining the lower content of H_2S in the tests at higher temperatures.

Tar contents were analysed with two instruments, an HPLC and a GC-MS; the results obtained for all the tests are compared in Fig. 3.

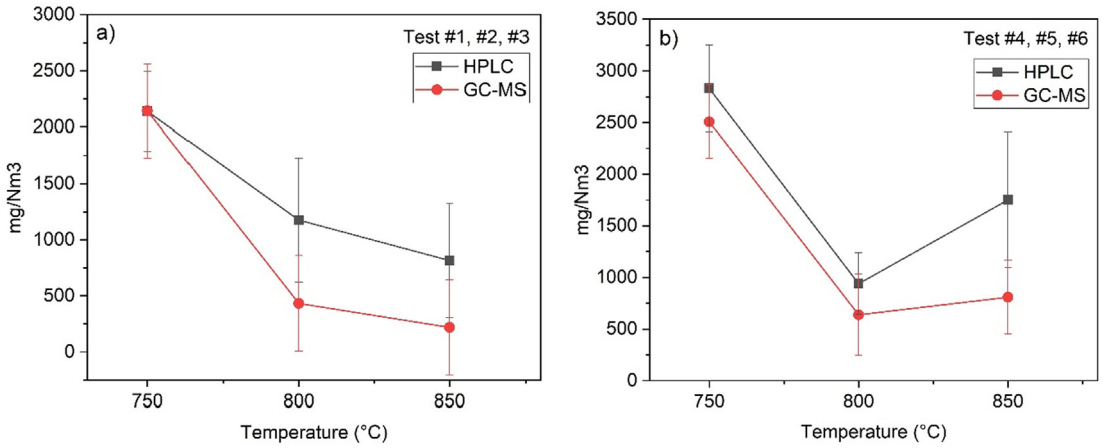

Fig. 3. Tar contents obtained with HPLC and GC-MS analysis in tests 1, 2, 3 (a) and tests 3, 4, 5 (b).

Table 3
Tar compounds analysed by GC-MS.

Test	#1	#2	#3	#4	#5	#6
				mg/Nm^3		
Toluene	979	120	29	1615	393	416
1-ring compounds	166	16	3	427	53	109
Naphthalene	824	183	83	405	156	200
2-ring compounds	71	73	60	44	31	45
3- and 4- ring compounds	13	34	43	10	4	31
Phenols	91	6	2	8	2	8

It shows that the tar contents obtained with the different analysis instruments give coherent results, reproducing the same trends from different tests. Tar contents obtained with HPLC have slightly higher values compared to the data given by GC-MS, however the results obtained with the two instruments are in the same order of magnitude and confirm the coherence of the analysis methods and the reliability of the obtained trends. Results in Fig. 3 highlight that for higher temperatures the tar contents are lower, due to the enhancement of thermal tar decomposition; values obtained for test #6 are the only points that do not comply with the decreasing trend observed for higher temperatures. Assuming that no contingent sampling or measurement issues occurred, this could be explained by the higher C conversion and gas yield of test #6 (as shown in Table 2) that would cause the development of lighter aromatic tar compounds in larger amount (see Table 3).

The tar compounds detected and quantified with the GC-MS are listed in Table 3. Except from toluene, naphthalene and phenols, the other tars are lumped in groups according to the number of their aromatic rings. Based on the compounds detected by the instrument, 1-ring compounds include styrene, xylene and indene; 2-ring compounds include acenaphthylene, acenaphthene and fluorene; 3- and 4- ring compounds include fluoranthene, pyrene, phenanthrene and anthracene.

The tar compositions displayed in Table 3 show that the heavier tar compounds (2-ring and higher) are present in very low quantities in all the 6 experimental runs. In tests carried out with SRF, the content of lighter tars is slightly higher compared to the equivalent data in tests without SRF, even if in the same order of magnitude. This observation is consistent with the results of gas compositions, in which the higher content of CH_4 obtained (and thus light hydrocarbons in general) was ascribed to the plastic material contained in the SRF, as also confirmed in literature (Pinto et al., 2007; Valin et al., 2019).

Overall, results obtained by mixing SRF with lignite show that the blend of the two materials in the proportion 20:80 wt% respectively, does not cause a significant increase in tar content, that have a maximum value of approximately 2800 mg/Nm^3 obtained at 750 °C, and also does not substantially impact on the product gas composition Therefore, the addition of 20 wt% of SRF to the lignite feedstock does not negatively affect the steam gasification process. Additionally, this proves the feasibility of steam gasification in fluidized bed reactors with the environmentally virtuous practice of SRF blending with a fossil carbonaceous feedstock.

3.3. Pressure fluctuations analysis

More than 50 acquisitions of pressure fluctuations were carried out during the experimental tests with lignite feedstock, in order to evaluate the bed fluidization quality. During the preliminary heating of the reactor, PSDF resulted in dominant frequencies around 2–3 Hz (Fig. 4**a**), which were compatible with the desired bubbling fluidization regime (characteristic frequencies lower than 10 Hz). When gasification started, a series of low-frequency phenomena (less than1 Hz) took action with high-power-spectral-density; these phenomena were associated to the peristaltic pump feeding water and to abrupt devolatilization of solid particles. Portions of PSDF from gasification sessions were associated to fluidization phenomena, with locally dominant frequencies between 3 and 4 Hz at 750 °C (Fig. 4**b**), 800 °C (Fig. 4**c**), 850 °C (Fig. 4**d**). Pressure fluctuations signals acquired after the gasification tests, when water and lignite were no longer fed, showed that the local dominant frequencies of bubbling bed returned within the range 2–3 Hz (an example in Fig. 4**d**), with residual disturbances at frequencies lower than 1 Hz. In general, the dominant value of the bed inventory was always in the range 2–4 Hz, well ascribable to a bubbling fluidization regime; this implies that bed particles did not undergo

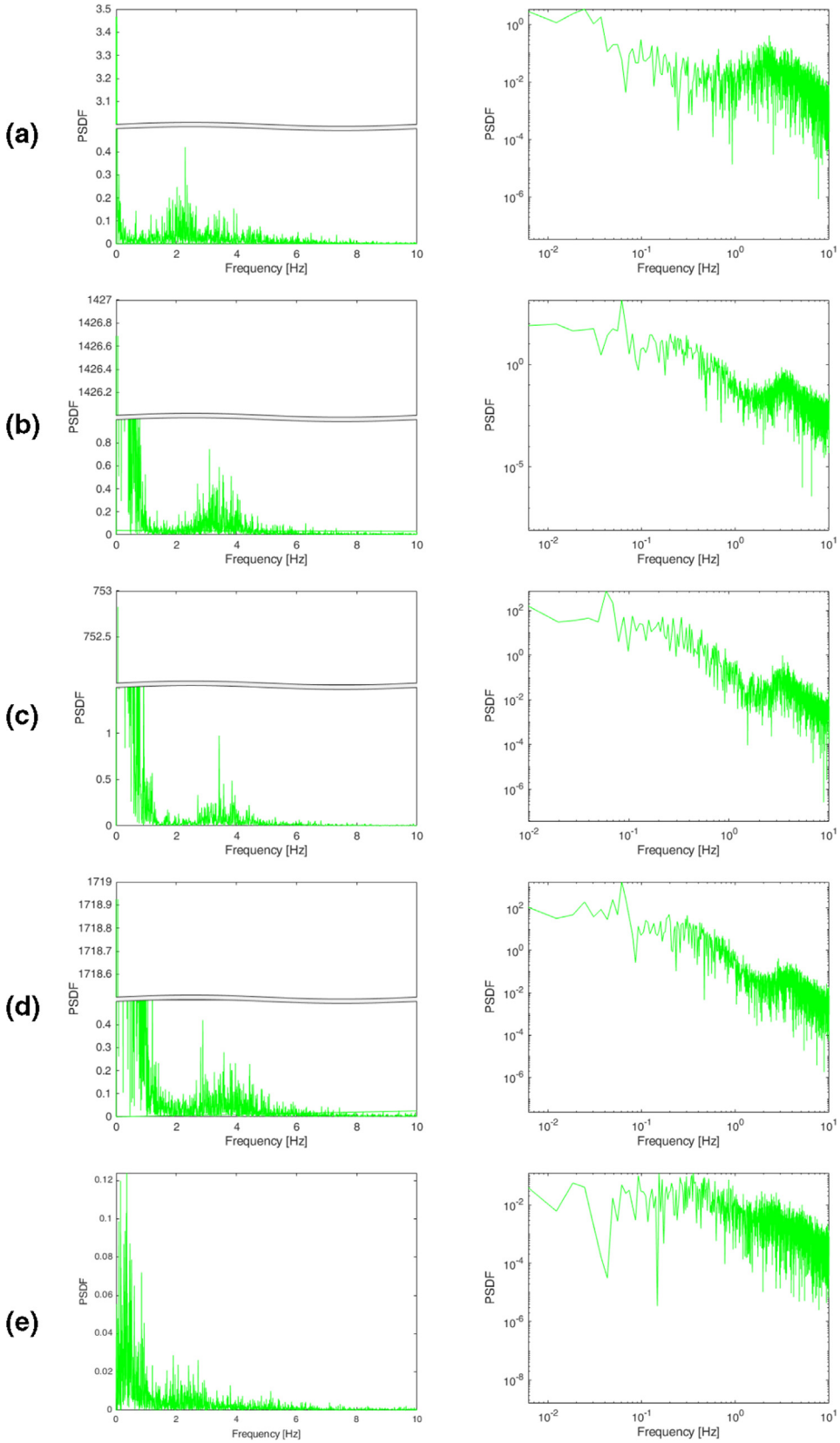

Fig. 4. PSDF of pressure fluctuations signals from tests with lignite as a feedstock, in linear (first column) and logarithmic (second column) scales: pre-heating under N_2, 735 °C (a), gasification at 750 °C (b); gasification at 800 °C (c), gasification at 850 °C (d), post-combustion after test at 850 °C (e).

modifications able to alter their fluidization quality, such as sintering or melting with ashes. The results obtained and the related comments, such as the low frequency phenomena observed when the feeding started, and the absence of power decay indicating no sign of defluidization, can be confirmed with other studies on processing of pressure fluctuation signals (Johnsson et al., 2000).

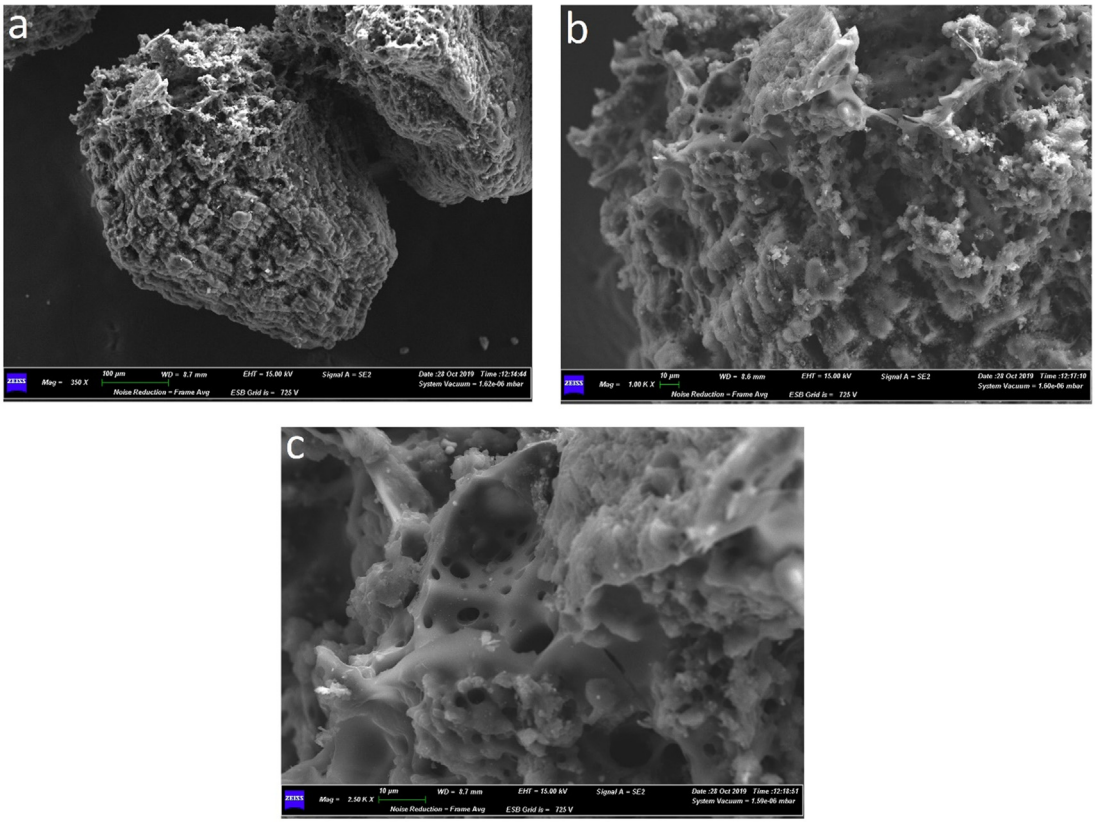

Fig. 5. SEM analysis of HTW bottom product after use. Magnification (a): 350x; (b): 1000x; (c): 2500x.

3.4. Analysis of materials after test

3.4.1. HTW bottom product after tests

Characterization analysis on the HTW bottom product was repeated after the 6 tests; the result of the particle size analysis on the HTW bottom product after use is shown in Fig. 1**S**.

The average $d_{3,2}$ diameter of HTW bottom product after tests is 109.02 μm, greatly reduced compared to its diameter before the tests. The lower particle size of the bed material suggests the absence of agglomeration phenomena, corroborating the inferences from pressure fluctuations analysis about the absence of de-fluidization phenomena. A possible cause of the reduction of the HTW bottom product particle size after tests is the attrition and erosion to which the particles are subject because of fluidization. Moreover, the particles during the tests could have lost part of their mass because of chemical conversion, i.e. their carbonaceous fraction may have participated in the gasification reactions, as also observed from the results of gas compositions.

The CHNS analysis on the sample of HTW bottom product was repeated after the gasification tests, the results are shown in Table 1: results show that the C content of the HTW bottom product after tests is slightly lower than that of the sample before use (Table 1). This C lowering in HTW bottom product particles is in agreement with the above-mentioned hypothesis of partial conversions during the gasification reactions.

The analysis of the HTW bottom product after use (standard ISO 1171:2010 (ISO, 2010)) gives an ash content of 34.32 wt%, much higher than the value of the material before the tests (9.48 wt%); probably this increased ash content is due to the accumulation in the bed material of the inorganic fraction of the feedstock during the gasification tests.

The use of HTW bottom product as bed material seems to be a good option for the gasification process, as observed from the high values of H_2O and C conversions, gas yield and CO content, especially at higher temperatures. This effect could be related to the ash contained in the bed material, which are rich in alkali compounds that are reported to have enhancing properties in steam gasification reactions (Yip et al., 2010).

HTW bottom product after the gasification tests was again analysed with SEM/EDS. The results are shown in Fig. 5.

The SEM images of the HTW bottom product after the gasification tests show a foam-like structure with several holes on the surface, particularly evident in Fig. 5**c**. The several channels on the surface and the spongy structure could have been caused by a mild release of gas from the material, due to the fact that the gasification tests were carried out with steam. This further corroborates the hypothesis of partial reactivity shown by HTW bottom product as a bed inventory.

4. Conclusions

Gasification tests were carried out in a bench-scale fluidized bed gasifier, with HTW bottom product as bed material, in order to reproduce the HTW gasification process. The effect of temperature was studied in tests with two solid feed options: simple lignite or a mixture of lignite and SRF, to assess the feasibility of co-gasification of waste in a fluidized bed reactor. The results obtained showed that higher operating temperatures determine a better quality of the produced gas, in terms of higher conversions, H_2 and CO contents, and lower tars content. Gasification of lignite-SRF mixture produced a gas with composition and tar content close to the outputs obtained in the gasification tests with simple lignite. In more detail, tar content, CH_4 and CO_2 concentrations were slightly higher in presence of SRF, probably because of its plastic fraction.

It was observed that the use of HTW bottom product in the gasifier produces high values of conversions and yields, probably because of the ash elements contained in the bed material that could enhance the gasification process; furthermore some of the C contained in the HTW bottom product probably participated to the gasification reaction, as observed by the gas composition and confirmed by the analysis of the material before and after the tests.

The pressure fluctuation analysis did not show signs of defluidization of the bed, and thus it was deduced that phenomena of ash melting, or agglomeration of the bed material did not take place during the gasification tests.

To conclude, these gasification tests on a bench-scale demonstrated that the addition of waste material to lignite does not cause relevant issues or substantial changes in the gas composition and tar production. It can be concluded that gasification of 20 wt% of SRF with lignite as feedstock and HTW bottom product as bed material, can be operated without issues or significant losses in gas quality. This points how lignite/SRF co-gasification is a workable process option for waste disposal.

Declaration of Competing Interest

The authors declare that they have no known competing financial interests or personal relationships that could have appeared to influence the work reported in this paper.

Acknowledgements

The authors kindly acknowledge the financial support of the European Project LIG2LIQ (RFCS-01-2017 n°796585) co-funded by the European Commission managed Research Fund for Coal and Steel (RFCS). The authors thank RWE Power AG for supplying lignite, TUDA for supplying HTW bottom product and N + P for supplying SRF. ICHPW is also kindly acknowledged for the characterization analysis of lignite and SRF. The authors thank Dr. Alessia Pepe from University of Teramo for the HPLC analyses, and Dr. Angela Rolfe from Ulster University for having proof-read the manuscript and corrected the English language.

Appendix A. Supplementary material

Supplementary data to this article can be found online at https://doi.org/10.1016/j.wasman.2020.07.016.

References

Arena, U., 2012. Process and technological aspects of municipal solid waste gasification. A review. Waste Manage. 32 (4), 625–639. https://doi.org/10.1016/j.wasman.2011.09.025.

Arena, Umberto, Di Gregorio, Fabrizio, 2014. Gasification of a solid recovered fuel in a pilot scale fluidized bed reactor. Fuel 117, 528–536. https://doi.org/10.1016/j.fuel.2013.09.044.

Arena, U., Di Gregorio, F., 2016. Fluidized bed gasification of industrial solid recovered fuels. Waste Manage. 50, 86–92. https://doi.org/10.1016/j.wasman.2016.02.011.

Arena, U., Di Gregorio, F., De Troia, G., Saponaro, A., 2015. A techno-economic evaluation of a small-scale fluidized bed gasifier for solid recovered fuel. Fuel Process. Technol. 131, 69–77. https://doi.org/10.1016/j.fuproc.2014.11.003.

Arena, U., Zaccariello, L., Mastellone, M.L., 2010. Fluidized bed gasification of waste-derived fuels. Waste Manage. 30 (7), 1212–1219. https://doi.org/10.1016/j.wasman.2010.01.038.

Basu, P., 2006. Combustion and Gasification in Fluidized beds. In CRC Press, CRC Press. https://doi.org/10.1201/9781420005158.

Belgiorno, V., De Feo, G., Della Rocca, C., Napoli, R.M.A., 2003. Energy from gasification of solid wastes. Waste Manage. 23 (1), 1–15. https://doi.org/10.1016/S0956-053X(02)00149-6.

Borgwardt, R.H., 1984. Reaction of H2S and Sulfur with limestone particles. Ind. Eng. Chem. Process Des. Dev. 23, 742–748. https://doi.org/10.1021/i200027a020.

Bosmans, A., Vanderreydt, I., Geysen, D., Helsen, L., 2013. The crucial role of Waste-to-Energy technologies in enhanced landfill mining: A technology review. J. Cleaner Prod. 55, 10–23. https://doi.org/10.1016/j.jclepro.2012.05.032.

Chang, L.P., Xie, Z.L., Xie, K.C., 2006. Study on the formation of NH 3 and HCN during the gasification of brown coal in steam. Process Safety Environ. Protect. 84 (6B), 446–452. https://doi.org/10.1205/psep05019.

Chen, N.Y., Yan, T.Y., 1986. M2 forming a process for aromatization of light hydrocarbons. Ind. Eng. Chem. Process Des. Develop. 25 (1), 151–155. https://doi.org/10.1021/i200032a023.

European Association for Coal and Lignite. (n.d.). EURACOAL statistics. https://euracoal.eu/info/euracoal-eu-statistics/

Eurostat, 2019. Waste statistics. https://ec.europa.eu/eurostat/statistics-explained/index.php?title=Waste_statistics

G.A. n°796585., 2018. LIG2LIQ Eu Project - web page. https://www.lig2liq.eu/.

Galloway, Benjamin D., Sasmaz, Erdem, Padak, Bihter, 2015. Binding of SO3 to fly ash components: CaO, MgO, Na2O and K2O. Fuel 145, 79–83. https://doi.org/10.1016/j.fuel.2014.12.046.

Gallucci, K., Gibilaro, L.G., 2005. Dimensional cold-modeling criteria for fluidization quality. Ind. Eng. Chem. Res. 44 (14), 5152–5158. https://doi.org/10.1021/ie049407t.

Gallucci, K., Jand, N., Foscolo, P.U., Santini, M., 2002. Cold model characterisation of a fluidised bed catalytic reactor by means of instantaneous pressure measurements. Chem. Eng. J. 87 (1), 61–71. https://doi.org/10.1016/S1385-8947(01)00202-9.

Herdel, P., Krause, D., Peters, J., Kolmorgen, B., Ströhle, J., Epple, B., 2017. Experimental investigations in a demonstration plant for fluidized bed gasification of multiple feedstock's in 0.5 MW th scale. Fuel 205, 286–296. https://doi.org/10.1016/j.fuel.2017.05.058.

Hervy, M., Remy, D., Dufour, A., Mauviel, G., 2019. Air-blown gasification of Solid Recovered Fuels (SRFs) in lab-scale bubbling fluidized-bed: Influence of the operating conditions and of the SRF composition. Energy Convers. Manage. 181, 584–592. https://doi.org/10.1016/j.enconman.2018.12.052.

Hu, Y., Watanabe, M., Aida, C., Horio, M., 2006. Capture of H2S by limestone under calcination conditions in a high-pressure fluidized-bed reactor. Chem. Eng. Sci. 61 (6), 1854–1863. https://doi.org/10.1016/j.ces.2005.10.006.

ISO, 2010. 1171:2010 Solid Mineral Fuels. Determination of Ash. European Committee for Standardization

Johnsson, F., Zijerveld, R.C., Schouten, J.C., Van Den Bleek, C.M., Leckner, B., 2000. Characterization of fluidization regimes by time-series analysis of pressure fluctuations. Int. J. Multiph. Flow 26 (4), 663–715. https://doi.org/10.1016/S0301-9322(99)00028-2.

Karimipour, S., Gerspacher, R., Gupta, R., Spiteri, R.J., 2013. Study of factors affecting syngas quality and their interactions in fluidized bed gasification of lignite coal. Fuel 103, 308–320. https://doi.org/10.1016/j.fuel.2012.06.052.

Krause, D., Herdel, P., Ströhle, J., Epple, B., 2019. HTW^{TM}-gasification of high volatile bituminous coal in a 500 kWth pilot plant. Fuel 250, 306–314. https://doi.org/10.1016/j.fuel.2019.04.014.

Lahijani, P., Zainal, Z.A., Mohammadi, M., Mohamed, A.R., 2015. Conversion of the greenhouse gas CO2 to the fuel gas CO via the Boudouard reaction: A review. Renew. Sustain. Energy Rev. 41, 615–632. https://doi.org/10.1016/j.rser.2014.08.034.

Li, C.Z., Tan, L.L., 2000. Formation of NOx and SOx precursors during the pyrolysis of coal and biomass. Part III. Further discussion on the formation of HCN and NH3 during pyrolysis. Fuel 79 (15), 1899–1906. https://doi.org/10.1016/S0016-2361(00)00008-9.

Lombardi, L., Carnevale, E., Corti, A., 2015. A review of technologies and performances of thermal treatment systems for energy recovery from waste. Waste Manage. 37, 26–44. https://doi.org/10.1016/j.wasman.2014.11.010.

Meylan, F.D., Moreau, V., Erkman, S., 2015. CO2 utilization in the perspective of industrial ecology, an overview. J. CO2 Util. 12, 101–108. https://doi.org/10.1016/j.jcou.2015.05.003.

N+P Subcoal®. (n.d.). https://www.subcoal-international.nl/.

Patel, C., Lettieri, P., Germanà, A., 2012. Techno-economic performance analysis and environmental impact assessment of small to medium scale SRF combustion plants for energy production in the UK. Process Saf. Environ. Prot. 90 (3), 255–262. https://doi.org/10.1016/j.psep.2011.06.015.

Pinto, F., André, R.N., Carolino, C., Miranda, M., Abelha, P., Direito, D., Perdikaris, N., Boukis, I., 2014. Gasification improvement of a poor quality solid recovered fuel (SRF). Effect of using natural minerals and biomass wastes blends. Fuel 117, 1034–1044. https://doi.org/10.1016/j.fuel.2013.10.015.

Pinto, F., Franco, C., André, R.N., Tavares, C., Dias, M., Gulyurtlu, I., Cabrita, I., 2003. Effect of experimental conditions on co-gasification of coal, biomass and plastics wastes with air/steam mixtures in a fluidized bed system. Fuel 82 (15–17), 1967–1976. https://doi.org/10.1016/S0016-2361(03)00160-1.

Pinto, F., Lopes, H., André, R.N., Gulyurtlu, I., Cabrita, I., 2007. Effect of catalysts in the quality of syngas and by-products obtained by co-gasification of coal and wastes. 1. Tars and nitrogen compounds abatement. Fuel 86 (14), 2052–2063. https://doi.org/10.1016/j.fuel.2007.01.019.

Qin, Y.H., Campen, A., Wiltowski, T., Feng, J., Li, W., 2015. The influence of different chemical compositions in biomass on gasification tar formation. Biomass Bioenergy 83, 77–84. https://doi.org/10.1016/j.biombioe.2015.09.001.

Recari, J., Berrueco, C., Abelló, S., Montané, D., Farriol, X., 2016. Gasification of two solid recovered fuels (SRFs) in a lab-scale fluidized bed reactor: Influence of experimental conditions on process performance and release of HCl, H2S, HCN and NH3. Fuel Process. Technol. 142, 107–114. https://doi.org/10.1016/j.fuproc.2015.10.006.

Savuto, E., Di Carlo, A., Steele, A., Heidenreich, S., Gallucci, K., Rapagnà, S., 2019. Syngas conditioning by ceramic filter candles filled with catalyst pellets and placed inside the freeboard of a fluidized bed steam gasifier. Fuel Process. Technol. 191, 44–53. https://doi.org/10.1016/j.fuproc.2019.03.018.

Savuto, E., May, J., Di Carlo, A., Gallucci, K., Di Giuliano, A., Rapagnà, S., 2020. Steam Gasification of Lignite in a Bench-Scale Fluidized-Bed Gasifier Using Olivine as Bed Material. Appl. Sci. 10 (8), 2931.

Singhabhandhu, A., Tezuka, T., 2010. The waste-to-energy framework for integrated multi-waste utilization: Waste cooking oil, waste lubricating oil, and waste plastics. Energy 35 (6), 2544–2551. https://doi.org/10.1016/j.energy.2010.03.001.

The World Bank, 2019. Solid Waste Management. https://www.worldbank.org/en/topic/urbandevelopment/brief/solid-waste-management.

Tian, F.J., Yu, J., McKenzie, L.J., Hayashi, J.I., Li, C.Z., 2007. Conversion of fuel-N into HCN and NH3 during the pyrolysis and gasification in steam: A comparative study of coal and biomass. Energy Fuels 21 (2), 517–521. https://doi.org/10.1021/ef060415r.

Tursun, Y., Liu, J., Xu, S., Wei, L., Zou, W., 2013. Catalytic steam gasification of lignite with olivine as solid heat carrier. Fuel 112, 641–645. https://doi.org/10.1016/j.fuel.2012.12.009.

Valin, S., Ravel, S., Pons de Vincent, P., Thiery, S., Miller, H., 2019. Fluidized bed air gasification of solid recovered fuel and woody biomass: Influence of experimental conditions on product gas and pollutant release. Fuel 242, 664–672. https://doi.org/10.1016/j.fuel.2019.01.094.

Venvik, H.J., Yang, J., 2017. Catalysis in microstructured reactors: Short review on small-scale syngas production and further conversion into methanol, DME and Fischer-Tropsch products. Catal. Today 285, 135–146. https://doi.org/10.1016/j.cattod.2017.02.014.

Wang, H., Pei, Y., Qiao, M., & Zong, B. (2017). Design of Bifunctional Solid Catalysts for Conversion of Biomass-Derived Syngas into Biofuels (pp. 137–158), Springer, Singapore. https://doi.org/10.1007/978-981-10-5137-1_4

Xie, K.C., Lin, J.Y., Li, W.Y., Chang, L.P., Feng, J., Zhao, W., 2005. Formation of HCN and NH33 during coal macerals pyrolysis and gasification with CO2. Fuel 84 (2–3), 271–277. https://doi.org/10.1016/j.fuel.2004.07.012.

Yip, K., Tian, F., Hayashi, J.I., Wu, H., 2010. Effect of alkali and alkaline earth metallic species on biochar reactivity and syngas compositions during steam gasification. Energy Fuels 24 (1), 173–181. https://doi.org/10.1021/ef900534n.

Zhou, J., Masutani, S.M., Ishimura, D.M., Turn, S.Q., Kinoshita, C.M., 2000. Release of fuel-bound nitrogen during biomass gasification. Ind. Eng. Chem. Res. 39 (3), 626–634. https://doi.org/10.1021/ie980318o.